Supplementary Information

1. Experimental Section

Synthesis of Au$_{24}$Ag$_{20}$(C$_{12}$H$_{13}$)$_{24}$Cl$_2$: AuSMe$_2$Cl was prepared according to literature methods.[S1] 60 mg AuSMe$_2$Cl and 30 mg CH$_3$COOAg were dissolved in 10 mL dichloromethane and 5 ml methanol. Then 1 mL of a methanol solution of 10 mg sodium methoxide and 30 μL 4-tert-butyl phenylacetylene were mixed together and sonicated for 5 minutes. Then the 4-tert-butyl phenylacetylene solution was added to the above solution under vigorous stirring. After 20 min, 10 mg tert-butylamineborane was added. The reaction was carried out at room temperature for 12 hours. After that, the reaction solution was centrifuged and the centrifugate precipitate was discarded, and the liquid was then washed with methanol several times to remove excess salts, alkynes and reducing agents. The target nanoclusters were extracted with dichloromethane. Finally, single crystal of Au$_{24}$Ag$_{20}$(C$_{12}$H$_{13}$)$_{24}$Cl$_2$ was obtained by diffusing methanol into toluene solution of the nanoclusters for two weeks.

Synthesis of Au$_{43}$Ag$_{38}$(C$_{12}$H$_{13}$)$_{36}$Cl$_{12}$: 60 mg AuSMe$_2$Cl and 30 mg CH$_3$COOAg were dissolved in 10 mL dichloromethane and 5 ml methanol. Then 1 mL of a methanol solution of 10 mg sodium methoxide and 30 μL 4-tert-butyl phenylacetylene were mixed together and sonicated for 5 minutes. Then the 4-tert-butyl phenylacetylene solution was added to the above solution under vigorous stirring. After 20 min, 10 mg tert-butylamineborane was added. The reaction was carried out at room temperature for 36 hours. After that, the reaction solution was centrifuged, the centrifugate precipitate was discarded, and the liquid was washed with methanol several times to remove excess salts, alkynes and reducing agents. The target nanoclusters were extracted with dichloromethane. Finally, single crystal of Au$_{43}$Ag$_{38}$(C$_{12}$H$_{13}$)$_{36}$Cl$_{12}$ was obtained by diffusing methanol into toluene solution of the nanoclusters for two weeks.

Synthesis of Au$_{24}$Ag$_{20}$(C$_9$H$_7$)$_{24}$Cl$_2$: 60 mg AuSMe$_2$Cl and 30 mg CH$_3$COOAg were dissolved in 10 mL dichloromethane and 5 ml methanol. Then 1 mL of a methanol solution of 10 mg sodium methoxide and 30 μL 2-methyl phenylacetylene were mixed

together and sonicated for 5 minutes. Then the 2-methyl phenylacetylene solution was added to the above solution under vigorous stirring. After 20 min, 20 μL diphenylsilane was added. The reaction was carried out at room temperature for 36 hours. After that, the reaction solution was centrifuged, the centrifugate precipitate was discarded, and the liquid was washed with methanol several times to remove excess salts, alkynes and reducing agents. The target nanoclusters were extracted with dichloromethane. Finally, single crystal of $Au_{24}Ag_{20}(C_9H_7)_{24}Cl_2$ was obtained by diffusing n-hexane into CH_2Cl_2 solution of the nanoclusters for two weeks.

Synthesis of $Au_{43}Ag_{38}(C_9H_7)_{36}Cl_9$: 60 mg $AuSMe_2Cl$ and 30 mg CH_3COOAg were dissolved in 10 mL dichloromethane and 5 ml methanol. Then 1 mL of a methanol solution of 10 mg sodium methoxide and 30 μL 2-methyl phenylacetylene were mixed together and sonicated for 5 minutes. Then the 2-methyl phenylacetylene solution was added to the above solution under vigorous stirring. After 20 min, 20 μL diphenylsilane was added. The reaction was carried out at room temperature for 36 hours. After that, the reaction solution was centrifuged, the centrifugate precipitate was discarded, and the liquid was washed with methanol several times to remove excess salts, alkynes and reducing agents. The target nanoclusters were extracted with dichloromethane. Finally, single crystal of $Au_{43}Ag_{38}(C_9H_7)_{36}Cl_9$ was obtained by diffusing n-hexane into CH_2Cl_2 solution of the nanoclusters for two weeks.

Characterization: The UV-vis absorption spectra with a range of 300-1000 nm were recorded on a UV-1800 spectrophotometer (Shimadzu, Japan). For $Au_{24}Ag_{20}(C_{12}H_{13})_{24}Cl_2$, $Au_{24}Ag_{20}(C_9H_7)_{24}Cl_2$ and $Au_{43}Ag_{38}(C_9H_7)_{36}Cl_9$, the diffraction data were collected on a Bruker D8 VENTURE with Mo Kα radiation (λ = 0.71073 Å). For $Au_{43}Ag_{38}(C_{12}H_{14})_{36}Cl_{12}$, the X-ray crystallography was performed on a Bruker D8 VENTURE with Ga Kα radiation (λ = 1.34139 Å). Electrospray ionization (ESI) mass spectra were collected on a Waters Q-TOF mass spectrometer using a Z-spray source. The $Au_{24}Ag_{20}(C_{12}H_{13})_{24}Cl_2$ sample was first dissolved in toluene (~ 0.5 mg/mL) and then diluted (2:1 v/v) with a methanol solution containing 50 mM $CsCO_3$. The $Au_{24}Ag_{20}(C_9H_7)_{24}Cl_2$ sample was first dissolved in toluene (~ 1 mg/mL) and then directly infused into the chamber at 5 μL/min. Chemical compositions of the

$Au_{43}Ag_{38}(C_{12}H_{13})_{36}Cl_{12}$ and $Au_{43}Ag_{38}(C_9H_7)_{36}Cl_9$ nanoclusters were determined by matrix-assisted laser desorption ionization time of flight (MALDI-TOF) mass spectrometry in positive-ion mode with trans-2-[3-(4-tert-Butylphenyl)-2-methyl-2-propenylidene]malononitrile (DCTB) as the matrix. A three-electrode system was employed for EIS (electrochemical impedance spectroscopy) experiments performed on a CHI660B electrochemical workstation, with working electrode (WE) of platinum foil, counter electrode (CE) of a glassy carbon and reference electrode of saturated Ag/AgCl. The experiments were carried out in 1 mol/L $KHCO_3$ at room temperature.

Catalytic test: All electrochemical tests were carried out in a customized H-type electrolytic cell, in which the anode and cathode compartments were separated by Nafion 117 membrane. The sample of each cluster uniformly coated on 1 cm×cm carbon paper (Toray TGP-H-090) was used as the working electrode, and the electrochemical workstation of Shanghai Chenhua CHI660D was used for electroreduction CO_2 test. Ag/AgCl electrode and platinum wire electrode were respectively used as reference electrode and counter electrode. Through $E_{RHE} = E_{Ag/AgCl} + 0.21\ V + 0.0591 \times pH$, all the electrode potentials in this study were converted to the reversible hydrogen electrode potential (RHE). The electrolyte was a 0.5 M $KHCO_3$ aqueous solution. Gas chromatography (GC) and nuclear magnetic resonance (NMR) techniques were selected to analyze the gas and liquid products, respectively.

Before the CO_2 electroreduction reaction, the $KHCO_3$ solution was purified with 30 mL/min CO_2 for 30 minutes to saturate the electrolyte and remove the air in the electrolytic cell. Linear voltammetry curve (LSV) was measured at a scanning rate of 10 mV/s from -0.3 to -1.2 V vs RHE at room temperature. During the reaction, the electrolyte in the cathode chamber was stirred at a speed of 300 rpm, and CO_2 gas was continuously and constantly introduced at a gas flow rate of 30 mL/min to purify and saturate it. The exhaust gas from the cathode chamber was analyzed at 20 min intervals using a gas chromatograph fitted with a thermal conductivity detector (TCD) and a hydrogen flame ionization detector (FID). The liquid product was detected by Bruker Avance 400 MHz ^{1}H NMR with dimethyl sulfoxide (DMSO) as the internal standard.

2. Computational Methods

All structural optimizations are implemented in ORCA5.0 quantum chemistry program package[S2] at the level of PBE/def2-SVP.[S3,S4] The calculation of single-point energy is instigated using higher-level PBE0/Def2-TZVP[S3] to obtain more accurate wave function information. The dispersion effect was considered in the structural optimization and calculations of single point energy by utilizes the atom-pairwise dispersion correction with the Becke-Johnson damping scheme (D3BJ).[S5,S6] It is worth mentioning that we use RI approximation in ORCA, so each basis set needs an auxiliary basis set, which can make the calculation easier when the accuracy sacrifice is negligible. In this study, Def2/J[S7] corresponding to the def2SVP and Def2-TZVP basis sets were used as auxiliary basis sets. In order to save computational resources, alkynyl groups have been simplified to methyl groups.

3. Supporting Figures and Tables
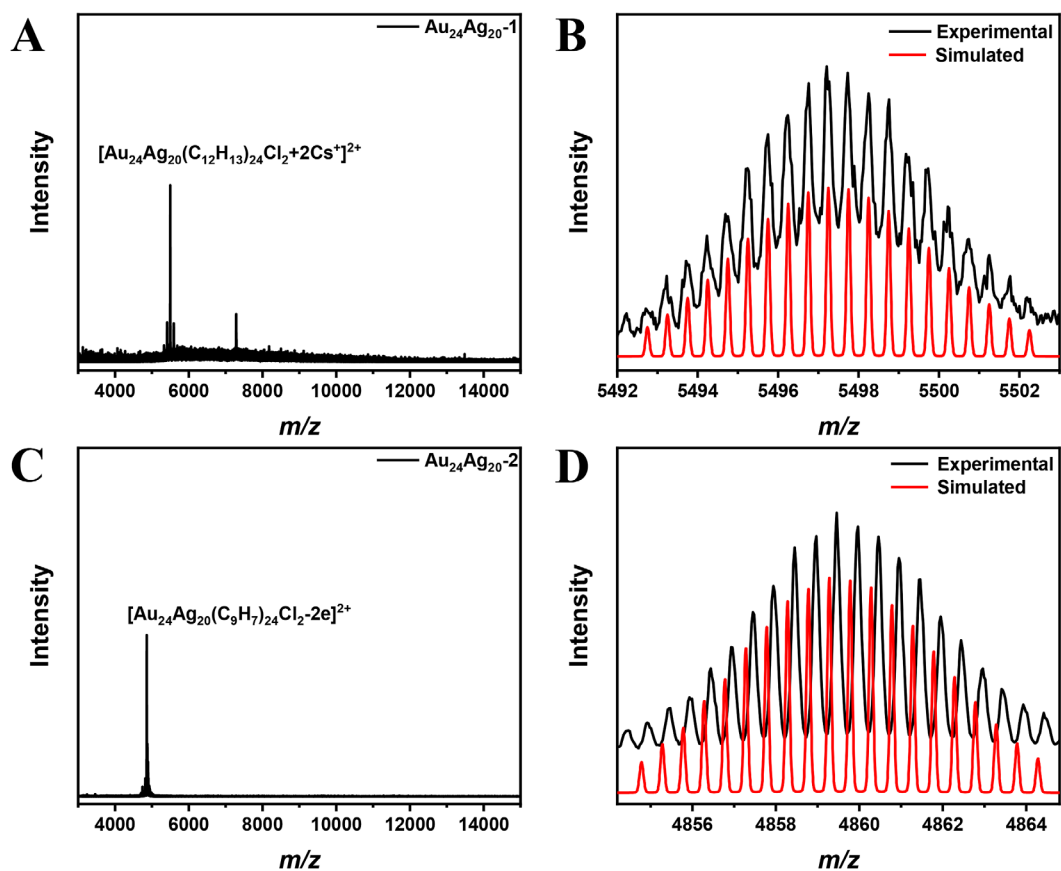
Fig. S1 (A) ESI-MS data for the $Au_{24}Ag_{20}(C_{12}H_{13})_{24}Cl_2$ nanocluster. (B) Comparison of the experiment and the simulated isotopic patterns of $Au_{24}Ag_{20}(C_{12}H_{13})_{24}Cl_2$ nanocluster. (C) ESI-MS data for the $Au_{24}Ag_{20}(C_9H_7)_{24}Cl_2$ nanocluster. (D) Comparison of the experiment and the simulated isotopic patterns of $Au_{24}Ag_{20}(C_9H_7)_{24}Cl_2$ nanocluster.
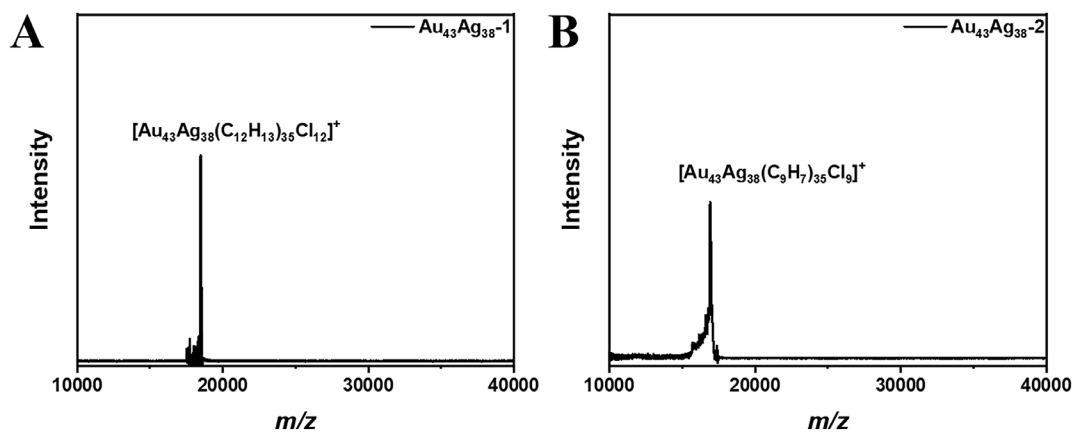
Fig. S2 MALDI-TOF-MS spectra of (A) $Au_{43}Ag_{38}(C_{12}H_{13})_{36}Cl_{12}$ and (B) $Au_{43}Ag_{38}(C_9H_7)_{36}Cl_9$. Note that the ESI-MS data of the two $Au_{43}Ag_{38}$ nanoclusters were difficult to be obtained and hence their MALDI-MS data were provided. Besides, one alkyne ligand for $Au_{43}Ag_{38}$ was removed during the MALDI-TOF-MS measurements.
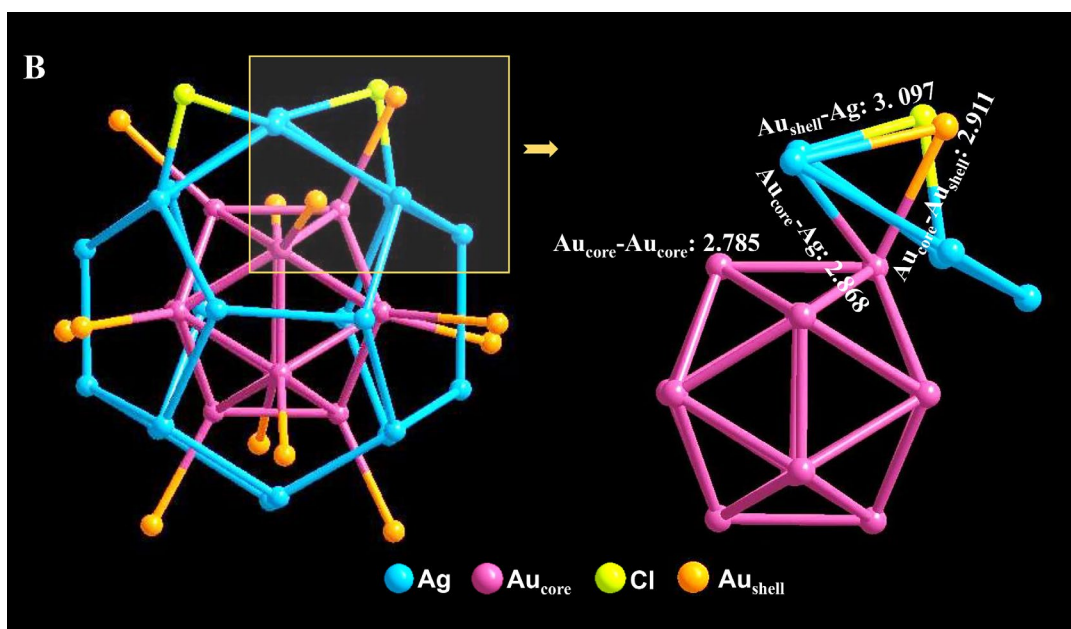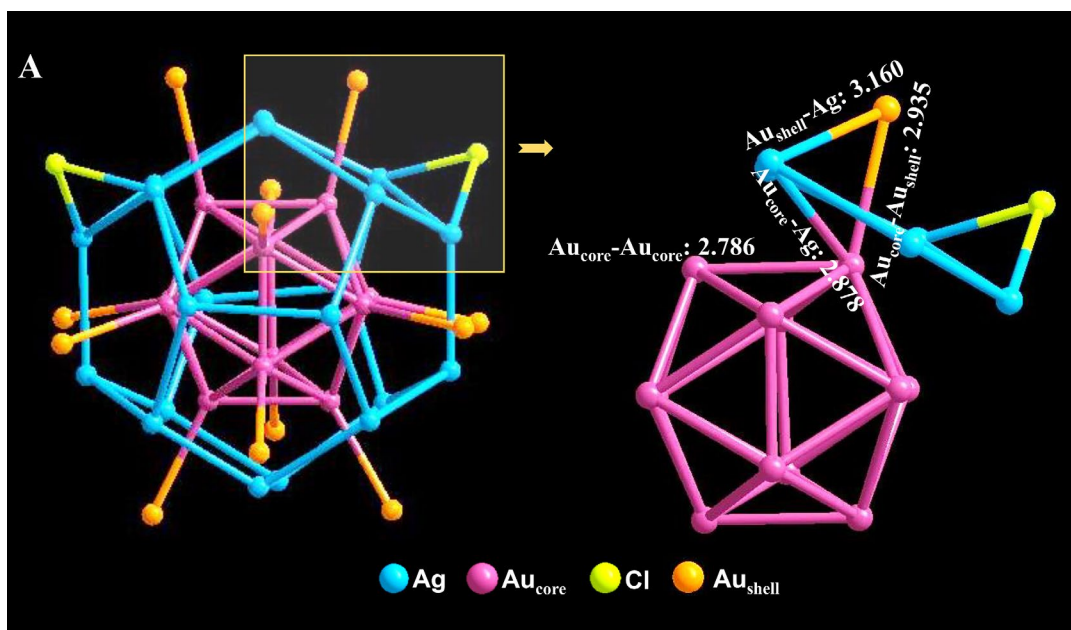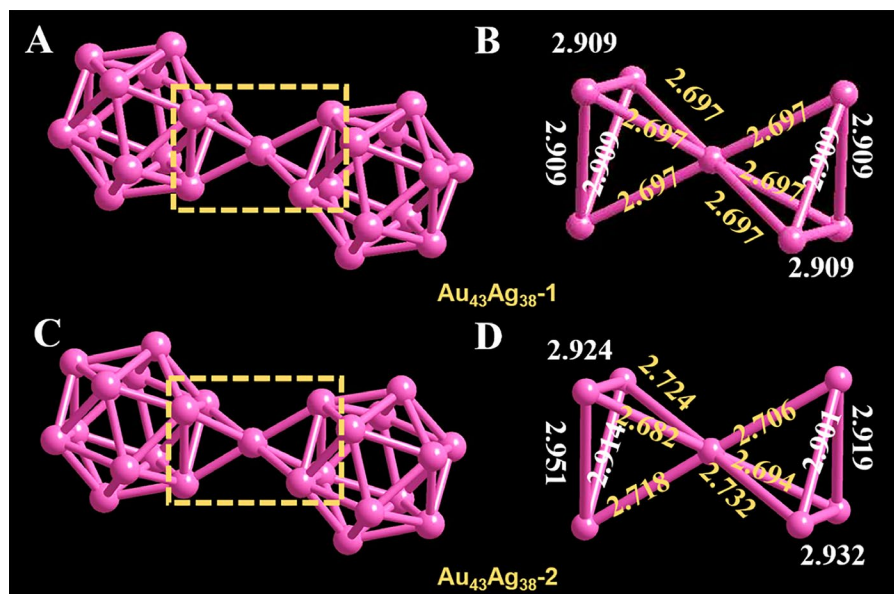
Fig. S3 Average bond lengths in (A) $Au_{24}Ag_{20}(C_{12}H_{13})_{24}Cl_2$ and (B) $Au_{24}Ag_{20}(C_9H_7)_{24}Cl_2$.
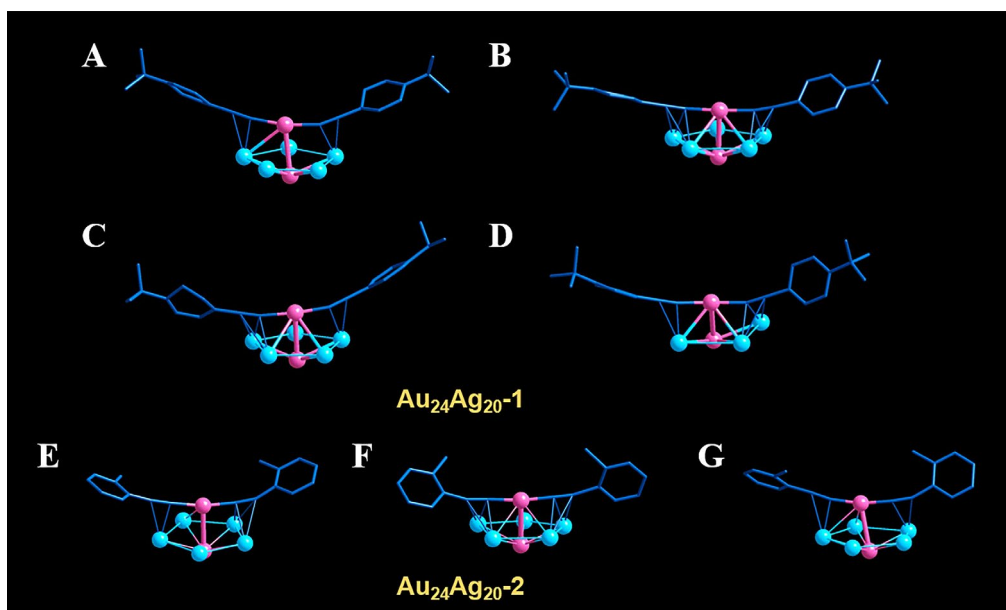
Fig. S4 Binding motifs in (A-D) $Au_{24}Ag_{20}(C_{12}H_{13})_{24}Cl_2$ and (E-G) $Au_{24}Ag_{20}(C_9H_7)_{24}Cl_2$.

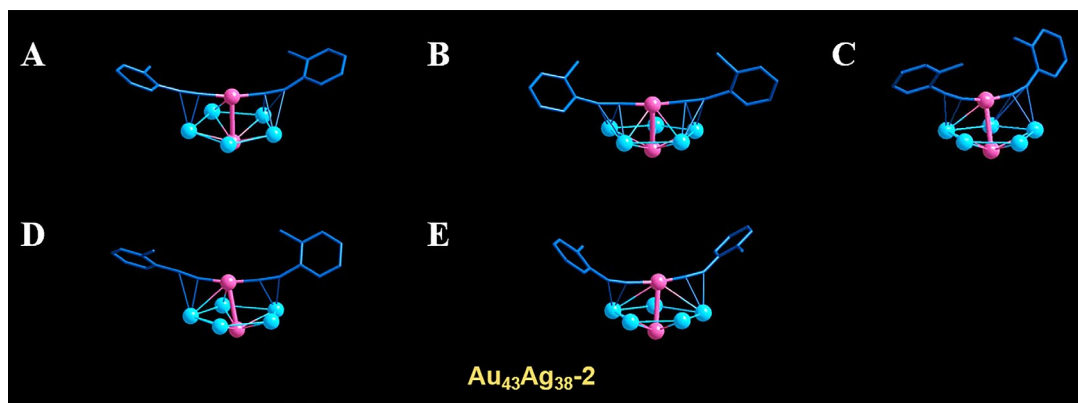**Fig. S5** Distances between the central Au atom and the neighbor Au atoms in (A, B) $Au_{43}Ag_{38}(C_{12}H_{13})_{36}Cl_{12}$ and (C, D) $Au_{43}Ag_{38}(C_9H_7)_{36}Cl_9$.
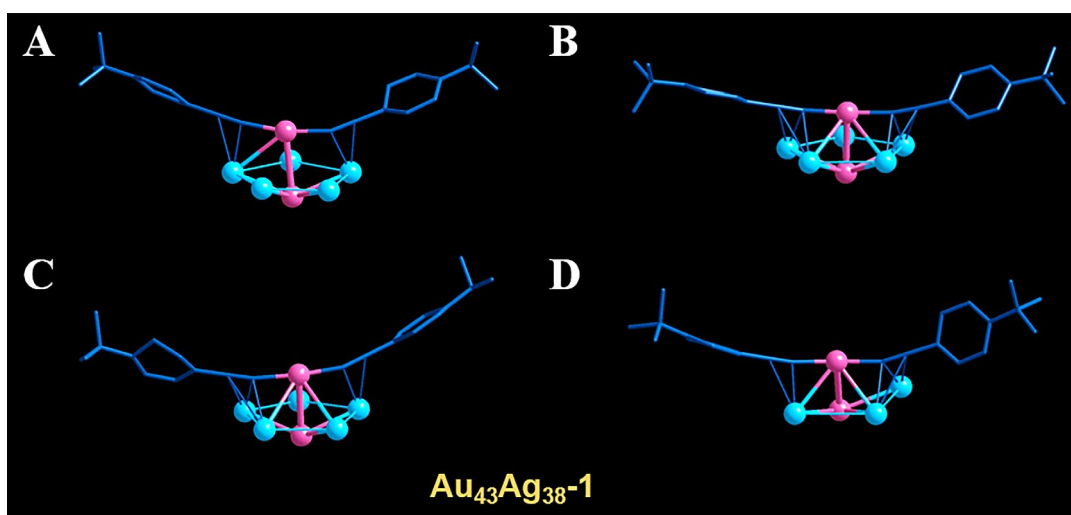
Fig. S6 Binding motifs in the $Au_{43}Ag_{38}(C_{12}H_{13})_{36}Cl_{12}$ nanocluster.

Fig. S7 Binding motifs in the Au₄₃Ag₃₈(C₉H₇)₃₆Cl₉ nanocluster.
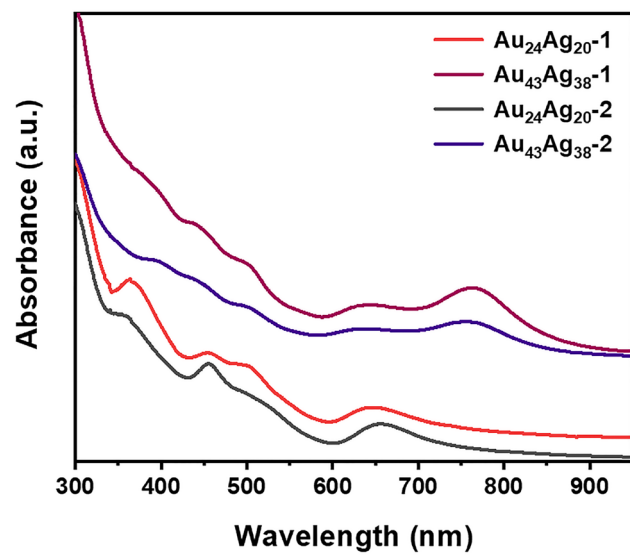
Fig. S8 UV-vis absorption spectra of the four nanoclusters.
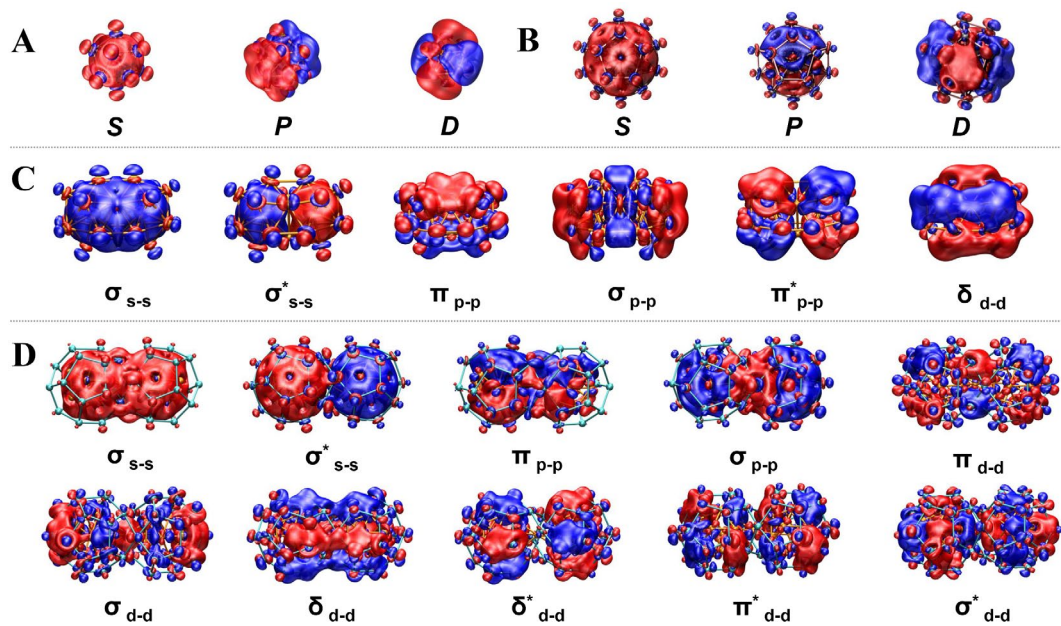
Fig. S9 Kohn-Sham MO diagrams of the inner cores of (A) $Au_{25}(SR)_{18}^-$, (B) $Au_{24}Ag_{20}$, (C) $Au_{38}(SR)_{24}$ and (D) $Au_{43}Ag_{38}$.
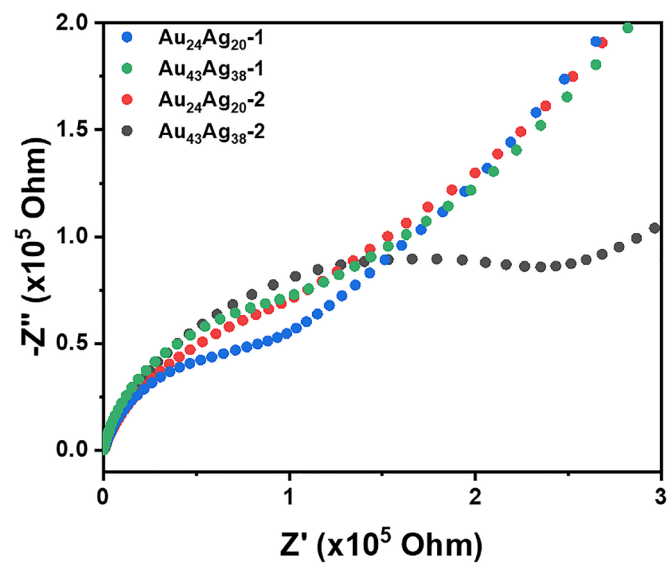
Fig. S10 The electrochemical impedance spectra (EIS) of the four clusters.

Table S1. Crystal data and structure refinement for the $Au_{24}Ag_{20}(C_{12}H_{13})_{24}Cl_2$ nanocluster.

Empirical formula	C288H312Ag20Au24Cl2
Formula weight	10728.854
Temperature	296(2) K
Wavelength	0.71073 Å
Crystal system	Triclinic
Space group	P -1
Unit cell dimensions	a = 19.2914(15) Å α = 97.077(2)°
	b = 24.9197(18) Å β = 105.131(2)°
	c = 34.987(3) Å γ = 100.118(2)°
Volume	15729(2) $Å^3$
Z	2
Density (calculated)	2.265 g/cm^3
Absorption coefficient	12.411 mm^{-1}
F(000)	9820
Theta range for data collection	2.003 to 24.034°.
Index ranges	-22<=h<=22, -29<=k<=28, -41<=l<=41
Reflections collected	110558
Independent reflections	24722 [R(int)= 0.0909]
Max. and min. transmission	0.370 and 0.190
Absorption correction	Multi-Scan
Refinement method	Full-matrix least-squares on F^2
Refinement program	SHELXL-2018/3(Sheldrick,2018)
Function minimized	$\Sigma\ w(F_o^2 - F_c^2)^2$
Data / restraints / parameters	55123 / 13854 / 3092
Goodness-of-fit on F^2	0.964
Δ/σ_{max}	0.010
Final R indices [I>2sigma(I)]	R1 = 0.0741, wR2 = 0.1757
R indices (all data)	R1 = 0.1685, wR2 = 0.2228
Largest diff. peak and hole	1.730 and -2.060 $eÅ^{-3}$

Table S2. Crystal data and structure refinement for the $Au_{43}Ag_{38}(C_{12}H_{13})_{36}Cl_{12}$ nanocluster.

Empirical formula	C864H942Ag76Au86Cl24
Formula weight	37314.16
Temperature	193(2) K
Wavelength	1.34139 Å
Crystal system	Trigonal
Space group	R -3
Unit cell dimensions	a = 26.1589(15) Å $\alpha = 90°$
	b = 26.1589(15) Å $\beta = 90°$
	c = 148.875(12) Å $\gamma = 120°$
Volume	88225(12) Å^3
Z	3
Density (calculated)	2.107 g/cm^3
Absorption coefficient	20.715 mm^{-1}
F(000)	50700
Theta range for data collection	1.716 to 59.599°.
Index ranges	-33<=h<=31, -33<=k<=31, -191<=l<=172
Reflections collected	356807
Independent reflections	43247 [R(int)=0.1214]
Absorption correction	Multi-Scan
Refinement method	Full-matrix least-squares on F^2
Refinement program	SHELXL-2018/3(Sheldrick,2018)
Function minimized	$\Sigma \ w(F_o{}^2 - F_c{}^2)^2$
Data / restraints / parameters	43247 / 6612 / 1550
Goodness-of-fit on F^2	1.014
Δ/σ_{max}	0.014
Final R indices [I>2sigma(I)]	R1 = 0.0714, wR2 = 0.1780
R indices (all data)	R1 = 0.1317, wR2 = 0.2160
Largest diff. peak and hole	2.492 and -2.559 eÅ^{-3}

Table S3. Crystal data and structure refinement for the $Au_{24}Ag_{20}(C_9H_7)_{24}Cl_2$ nanocluster.

Empirical formula	C216H168Ag20Au24Cl4
Formula weight	9789.89
Temperature	296(2) K
Wavelength	0.71073 Å
Crystal system	Triclinic
Space group	P -1
Unit cell dimensions	a = 18.9562(18) Å α = 78.295(3)°
	b = 19.6527(18) Å β = 79.704(3)°
	c = 33.671(3) Å γ = 63.881(2)°
Volume	10971.6(18) $Å^3$
Z	2
Density (calculated)	2.963 g/cm^3
Absorption coefficient	17.801 mm^{-1}
F(000)	8736
Theta range for data collection	1.995 to 25.000°.
Index ranges	-22<=h<=22, -23<=k<=22, -40<=l<=30
Reflections collected	72467
Independent reflections	38173 [R(int)=0.0688]
Max. and min. transmission	0.269 and 0.125
Absorption correction	Multi-Scan
Refinement method	Full-matrix least-squares on F^2
Refinement program	SHELXL-2018/3(Sheldrick,2018)
Function minimized	$\Sigma\ w(F_o{}^2 - F_c{}^2)^2$
Data / restraints / parameters	38173 / 11173 / 2339
Goodness-of-fit on F^2	1.025
Δ/σ_{max}	0.013
Final R indices [I>2sigma(I)]	R1 = 0.0882, wR2 = 0.2220
R indices (all data)	R1 = 0.1430, wR2 = 0.2571
Largest diff. peak and hole	4.088 and -2.860 $eÅ^{-3}$

Table S4. Crystal data and structure refinement for the $Au_{43}Ag_{38}(C_9H_7)_{36}Cl_9$ nanocluster.

Empirical formula	C324H251Ag38Au43Cl9
Formula weight	17031.90
Temperature	296(2) K
Wavelength	0.71073 Å
Crystal system	Triclinic
Space group	P -1
Unit cell dimensions	a = 25.413(2) Å α = 77.099(3)°
	b = 25.542(2) Å β = 83.178(3)°
	c = 28.705(3) Å γ = 73.626(3)°
Volume	17395(3) Å^3
Z	2
Density (calculated)	3.252 g/cm^3
Absorption coefficient	20.240 mm^{-1}
F(000)	15062
Theta range for data collection	1.952 to 25.359°.
Index ranges	-30<=h<=30, -29<=k<=30, 0<=l<=34
Reflections collected	60772
Independent reflections	25714 [R(int)=0.0514]
Max. and min. transmission	0.237 and 0.107
Absorption correction	Multi-Scan
Refinement method	Full-matrix least-squares on F^2
Refinement program	SHELXL-2018/3(Sheldrick,2018)
Function minimized	$\Sigma\ w(F_o{}^2 - F_c{}^2)^2$
Data / restraints / parameters	60772 / 15244 / 3677
Goodness-of-fit on F^2	1.053
Δ/σ_{max}	0.007
Final R indices [I>2sigma(I)]	R1 = 0.0912, wR2 = 0.1983
R indices (all data)	R1 = 0.2172, wR2 = 0.2526
Largest diff. peak and hole	2.815 and -2.771 eÅ^{-3}

Supporting References

S1 N. Nishina, Y. Yamamoto, *Synlett* **2007**, *11*, 1767.

S2 F. Neese, Software update: the ORCA program system, version 4.0. *WIREs Comput. Mol. Sci.* **2017**, *8*, e1327.

S3 J. P. Perdew, K. Burke, M. Ernzerhof, *Phys. Rev. Lett.* **1996**, *77*, 3865-3868.

S4 F. Weigend, R. Ahlrichs, *Phys. Chem. Chem. Phys.* **2005**, *7*, 3297-3305.

S5 S. Grimme, S. Ehrlich, L. Goerigk, *J. Comput. Chem.* **2011**, *32*, 1456-1465.

S6 S. Grimme, J. Antony, S. Ehrlich, *J. Chem. Phys.* **2010**, *132*, 154104.

S7 F. Weigend, *Phys. Chem. Chem. Phys.* **2006**, *8*, 1057-1065.